

# Hamiltonian analysis applied to the dynamic crack growth and arrest in a Double Cantilever Beam.

**Gilles DEBRUYNE<sup>1,\*</sup>, Radhi ABDELMOULA<sup>2</sup>**

<sup>1</sup> LaMSID-EDF-CEA, 1 avenue du Gal de Gaulle 92141 Clamart, France

<sup>2</sup> Paris XIII University, LSPM, Avenue J.B. Clément 93430 Villetaneuse, France

\* Corresponding author: [gilles.debruyne@edf.fr](mailto:gilles.debruyne@edf.fr)

---

## Abstract

The paper deals with the dynamic crack growth and arrest in an elastic DCB specimen, idealized by a Bernoulli-Euler beam. The surface energy of the material is  $2\Gamma_1$  and the initial crack is blunted with the energy  $2\Gamma_0 > 2\Gamma_1$ . The crack is then pushed ahead while the loading is frozen, the crack velocity and arrest length depending on the ratio  $R = \Gamma_0 / \Gamma_1$ . The analytical approach used to investigate the beam behaviour and the crack growth, is based on the Hamilton's principle of stationary action, considering an approximate equation of motion, based on a  $N$  modes decomposition of the beam deflection. This process leads to a set of  $N$  second order differential equations where the unknowns are the mode amplitudes and their derivatives, coupled to a single equation exhibiting the current crack length  $l(t)$ , velocity  $\dot{l}(t)$  and acceleration  $\ddot{l}(t)$ . The results concerning the crack kinematics, particularly the arrest length, are in good accordance with those obtained by a Finite Element Model associated to a cohesive zone model. The method is then applied to a material with heterogeneous fracture properties, in particular with a distribution of small brittle flaws perturbing the crack kinematics. This method allows a large range of configurations with a low computational time.

**Keywords** Crack arrest, Hamiltonian, Lagrange equations, Double Cantilever Beam, pops-in

---

## 1. Introduction

The double cantilever beam (DCB) specimen is widely used for crack arrest investigations, and its geometry is suitable for one-dimensional analysis models. For dynamic crack growth in a finite solid, analytical solutions are uncommon. The first quantitative prediction for the kinematics of a fast propagating crack, using an energy balance, is due to Mott [1]. Whereas crack propagation problems with transient motion are often achieved only with Finite Element Models, some analytical procedures are available for one dimensional models as DCB specimens. We focus here on a bimaterial DCB specimen, with a high toughness part where the initial crack is blunted, welded to a low toughness section where the crack enters with a high velocity. Transient kinetic analyses may be also achieved with some analytical methods, such hyperbolic equations solved by a finite difference scheme applied to characteristic lines [2,3]. An original analytical way, based on solving Lagrange's equation of a DCB specimen motion, considered as a Bernoulli-Euler beam, has been initiated by Burns and Webb [4], assuming a special form of the kinetic energy corresponding to a specific constant loading rate. Freund [5] has extended this approach for a general loading,

suggesting a modal decomposition, but limiting his work to the mode  $N = 0$ . It is suggested here to extend the modal analysis to higher vibration modes to investigate the dynamic crack growth and arrest in a DCB specimen.

## 2. The Bernoulli beam model applied to a duplex DCB.

An elastic Double Cantilever Beam specimen is illustrated in the figure 1. The specimen arms are slowly prescribed to a monotonic opening displacement  $W^0(t)$  which gives rise to a quasi-static mode I crack growth (denoted by the current value  $l_0 \leq l < l_c$ ) in a first part of the beam, made up of a  $2\Gamma_0$  surface energy material. A second material with a lower toughness, denoted the test section, is welded to the first one (the corresponding surface energy is  $2\Gamma_1 < 2\Gamma_0$ ). When the crack tip reaches the critical point corresponding to the sections interface ( $x = l_c$ ) where the toughness jump occurs, it rapidly runs throughout the test section, while the loading is frozen. The crack velocity  $\dot{x}$  (and the arrest length  $l_A$ ) in this test section, is governed by the surface energy ratio of the two sections ( $R = \Gamma_0 / \Gamma_1, R > 1$ ). We investigate here the crack kinematics during this stage, including the crack arrest  $l_c \leq x \leq l_A$ , with the assumption of a straight crack path, without any branching or kinking.

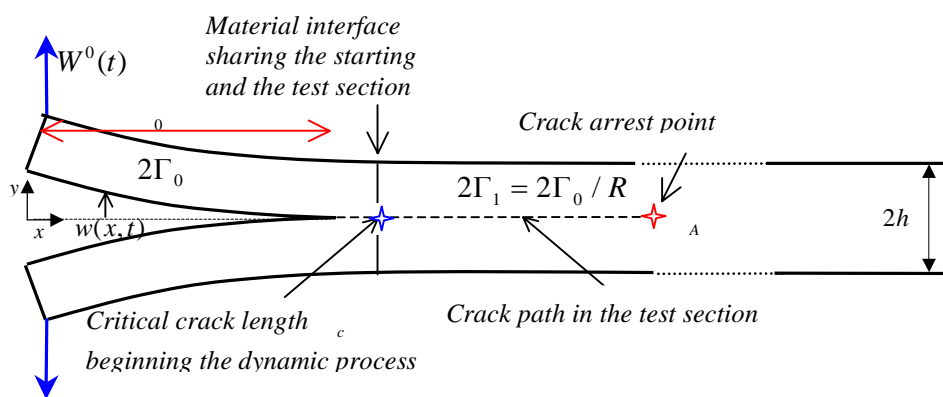


Figure 1 Crack growth and arrest in a bimaterial DCB specimen.

Only half of the specimen, and then half of the surface energy ( $\Gamma_0, \Gamma_1$ ) are considered here. A Bernoulli-Euler model is assumed to model the beam (the ratio  $h/l_c$  is considered small enough

to bear out a classical beam theory). Therefore, the motion only exhibits the scalar beam deflection  $w(x,t)$ . The general differential motion equation, associated with the boundary conditions may be written as follows,  $\forall l, 1_0 \leq l \leq 1_a$  :

$$\begin{cases} EI \frac{\partial^4 w}{\partial x^4} + \rho A \frac{\partial^2 w}{\partial t^2} = 0, & \forall x \in [0,1], \forall t \\ w(0,t) = W^0(t), \frac{\partial^2 w}{\partial x^2}(0,t) = 0, \\ w(1,t) = 0, \frac{\partial w}{\partial x}(1,t) = 0, \end{cases} \quad (1)$$

where  $E, I, A, \rho$  are respectively the elastic modulus, the area moment of inertia of the beam cross section, the area of this section, and the mass density of the material.

As the dynamic stage is the only one which matters, the initial conditions will refer to the crack running onset time when  $l(t=0) = l_c$ , so that the quasi-static growth stage ( $t < 0, x \in [0, l_c]$ ) is disregarded here.

### 3. Approximate equation of the DCB motion by modal decomposition

#### 3.1. Approximate equation of motion.

It is supposed, as already suggested by Freund [5], that the deflection of the beam is given by the following approximation :

$$w(X(t), t) = w^{stat}(X) + \hat{w}(X, t) = w^{stat}(X) + a_i(t) \phi_i(X), \quad i = 1, N \quad (2)$$

where the Einstein summation convention is henceforth adopted, from now on. The new variable  $X = x/l, X \in [0,1]$  is the normalized beam coordinate, useful in the case of a growing crack, such that the moving integration domain  $[0, l(t)]$  is replaced by the stationary reference domain  $[0,1], \forall l(t)$ .  $w^{stat}(X)$  is the quasi-static deflection solution,  $\hat{w}(X, t)$  the perturbation around the equilibrium solution,  $\phi_i$  the  $i^{\text{th}}$  normal mode shape for free vibration of the beam, and  $a_i$  the unknown deflection amplitude associated to  $\phi_i$ .

The homogeneous boundary conditions associated to the free vibration of the beam are derived from (1) :

$$\begin{cases} \phi_i(1) = \phi_i'(1) = 0, \\ \phi_i''(0) = \phi_i(0) = 0, \quad \forall i = 1, N \end{cases} \quad (3)$$

### 3.2. Free vibration mode shape.

An harmonic motion for the free vibration mode is assumed :

$$\hat{w}(X, t) = \phi_i(X) \sin(\omega_i t + \theta), \quad i = 1, N \quad (4),$$

where  $\omega_i$  is the angular frequency associated to the mode  $\phi_i$ ,  $\theta$  the phase angle.

The motion equation may be written as :

$$\phi_i^{(4)}(X) = \mu_i^4 \phi_i(X), \quad \forall i, i = 1, N, \quad \forall X \in [0, 1], \mu_i^4 = \frac{\rho A l^4 \omega_i^2}{EI} \quad (5)$$

The general solution of (10) is :

$$\phi_i(X) = \left[ \sin(\mu_i X) - \frac{\cos(\mu_i)}{\operatorname{sh}(\mu_i)} \operatorname{sh}(\mu_i X) \right] \quad (6)$$

and each angular frequency is given by the following equation:

$$\operatorname{tg}(\mu_i) = \operatorname{th}(\mu_i), \quad \forall i, i = 1, N \quad (7)$$

## 4. Hamilton's principle applied to a domain with a moving crack.

Hamilton's principle of stationary action is widely used in classical mechanics [6]. It postulates that the dynamics of a system is governed by a variational problem for a functional integrating the Lagrangian function, which contains some information about the energy of the system and the forces acting on it. It is the weak form of the differential equations of motion of the system.

### 4.1. General Hamilton's principle applied to a system described by a discrete set of degrees of freedom.

Let us recall the outlines of the principle for a system described by the generalized coordinates  $(q_i), i = 1, N$ , in a formal way. Hamilton's principle states that the true evolution of  $(q_i)$  along a path  $\gamma$  between two mechanical states at time  $t_0$  and  $t_1$  is a stationary point of the action

functional :  $\varphi(\gamma) = \int_{t_0}^{t_1} L(q_i, \dot{q}_i, t) dt$  (8), where  $L(q_i, \dot{q}_i, t)$  is the Lagrangian function of the system.

This principle involves the following system of  $N$  Euler-Lagrange equations [6] :

$$\frac{\partial L}{\partial q_i} - \frac{d}{dt} \frac{\partial L}{\partial \dot{q}_i} = 0, \quad \forall i, i = 1, N \quad (9)$$

Let us introduce the Hamiltonian function as the Legendre transform of the Lagrangian function :

$$H(q_i, p_i, t) = p_i \dot{q}_i - L(q_i, \dot{q}_i, t), \quad 1 \leq i \leq N \quad (10)$$

with  $p_i = \frac{\partial L}{\partial \dot{q}_i}$ . The following relations :

$$\dot{q}_i = -\frac{\partial H}{\partial p_i}, \quad \dot{p}_i = \frac{\partial H}{\partial q_i} \quad (11)$$

are called Hamilton's equations. The system of Euler-Lagrange's equations (14) is equivalent to the Hamilton's equations (16) (under some assumptions).

#### 4.2. Application to the DCB specimen.

These previous considerations are very formal and general. They can be applied to an elastodynamic system such our model, considering that  $q_i = a_i$ ,  $i = 1, N, q_{N+1} = 1$ . Therefore, the Lagrangian is :

$$\mathcal{L}(a_i, \dot{a}_i, 1, \dot{1}) = K(a_i, \dot{a}_i, 1, \dot{1}) - U(a_i, 1) - \int_0^1 \Gamma(x) dx, \quad i = 1, N \quad (12)$$

and the Euler-Lagrange equations become :

$$\frac{d}{dt} \left( \frac{\partial (K-U)}{\partial \dot{a}_i} \right) - \frac{\partial (K-U)}{\partial a_i} = 0, \quad \forall i, 1 \leq i \leq N \quad (13)$$

$$\frac{d}{dt} \left( \frac{\partial (K-U)}{\partial \dot{1}} \right) - \frac{\partial (K-U)}{\partial 1} + \Gamma(1) = 0, \quad (14)$$

which are respectively the local motion equations similar to equ. (1) for each eigenmode and the expression of the energy release rate. Using the Legendre transform of  $L$ , the following relation holds :

$$\mathcal{H}(a_i, \dot{a}_i, 1, \dot{1}) = K(a_i, \dot{a}_i, 1, \dot{1}) + U(a_i, 1) + \int_0^1 \Gamma(x) dx, \quad i = 1, N \quad (15)$$

Thus, the Hamiltonian is the total energy of the beam. Furthermore, since the Lagrangian equations are fulfilled, the energy balance is fulfilled. Starting from now, the complete solution of the dynamic crack growth problem in the DCB is restricted to the determination of the time dependent variables  $a_i(t), 1(t)$

## 5. Setting up the equations system, starting from the Hamilton's principle.

The relations (13) associated to the modal decomposition lead to the following second order ordinary differential system of  $N$  equations, describing the beam motion :

$$\ddot{w}_i = \frac{1}{I} (C_3^i + a_j C_4^{ij}) + \frac{2\Gamma}{I} \dot{w}_j C_4^{ij} + \frac{\Gamma^2}{I^2} (C_2^i + a_j C_1^{ij}) - \frac{1}{I^4} \frac{EI}{\rho A} a_i \mu_i^4, \forall i = 1, N \quad (16)$$

where  $(a_i, \dot{w}_i, \ddot{w}_i, i = 1, N)$  are the unknowns and  $(I, \Gamma, \rho A)$  the equation parameters. The coefficients  $(C_1^{ij}, C_2^i, C_3^i, C_4^{ij})$  depend on the mode shape of the beam, and  $\mu_i$  corresponds to the angular frequency computed with the relation (7). The relation (14) leads to the single equation, describing the crack kinematics (where the summation convention holds) :

$$\ddot{w} = \frac{\Gamma}{2I} + \frac{\Gamma}{\Delta} (-2\dot{w}_j C_2^j - 2\dot{w}_j a_i C_1^{ij}) + \frac{3EI}{2I^3 \Delta \rho A} (3(w^c)^2 + a_i^2 \mu_i^4) + \frac{1}{\Delta} \left( \dot{w}_j C_3^i + \dot{w}_j a_j C_4^{ij} - \frac{\Gamma_1}{2\rho A} \right) \quad (17)$$

with  $\Delta = \frac{6(w^c)^2}{35} + a_i a_j C_1^{ij} + 2a_i C_2^i$  and  $(I, \Gamma, \rho A)$  are the unknowns and  $(a_i, \dot{w}_i, \ddot{w}_i, i = 1, N)$  the equation parameters. It is important to point out that the above coupled system does not take into account two features : the irreversibility of the crack growth ( $\dot{w} \geq 0$ ) and the non overlap of the crack lips ( $w(x, t) \geq 0$ ), involving constraints on the amplitudes  $a_i$ , are not considered. This lack in the model will not affect the results in most of the cases as we will see in the next sections.

## 6. Application to an homogeneous test material

### 6.1. Number of modes influence.

The surface energy ratio is  $R = 3$ . From  $N = 3$ , the crack growth solution convergence may be considered as correct (with some oscillations, related to the propagation reversibility, see fig. 2).

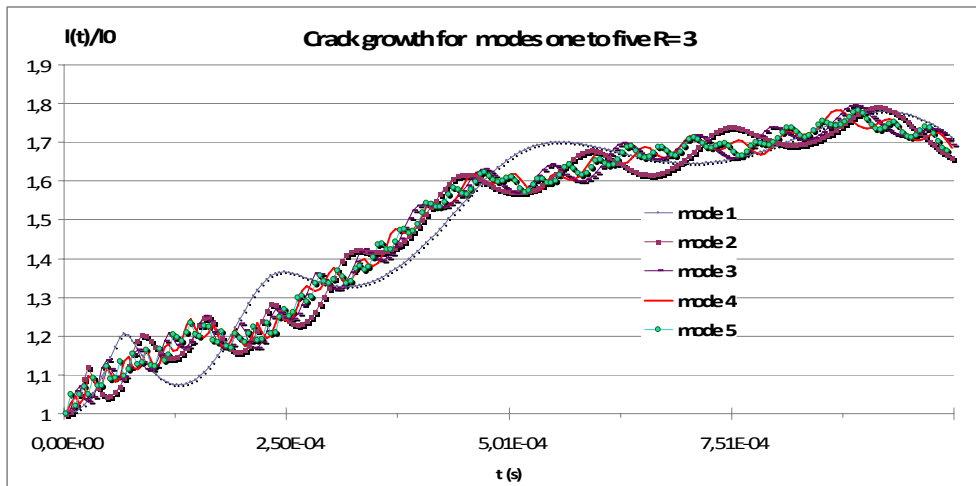


Fig. 2. Crack kinematics for a modal decomposition up to 5 modes ( $R=3$ ).

The crack arrest point arises as soon as the solution globally decreases.

## 6.2. Comparison with a cohesive zone model.

Our method has been compared with a cohesive zone model with a sufficiently small cohesive zone, to be close to the Griffith model [7] . Furthermore, this cohesive model is applied to a plane strain behavior while the present method uses a beam model. The comparative results from the present model and the cohesive model for  $R = 3$  are illustrated on the figures 3 and 4. The results (for  $N=4$ ) are in a good accordance. The crack arrest takes place when the kinetic energy reaches its minimum, before a second bounce, which corresponds to the beam vibration at the end of the crack propagation.

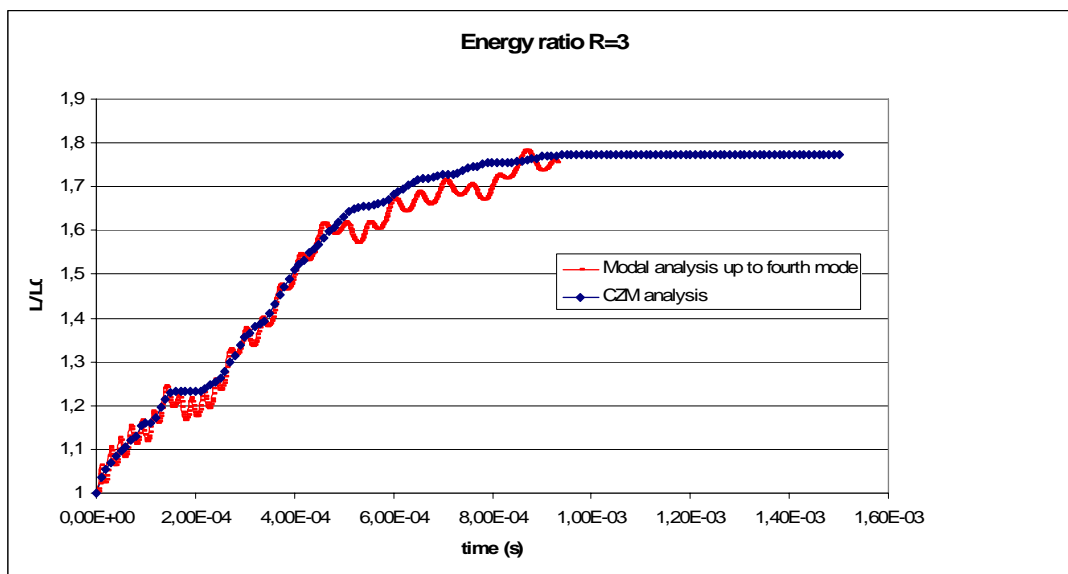


Fig. 3. Comparative analysis with a cohesive zone model :Crack kinematics versus time for  $R=3$ .

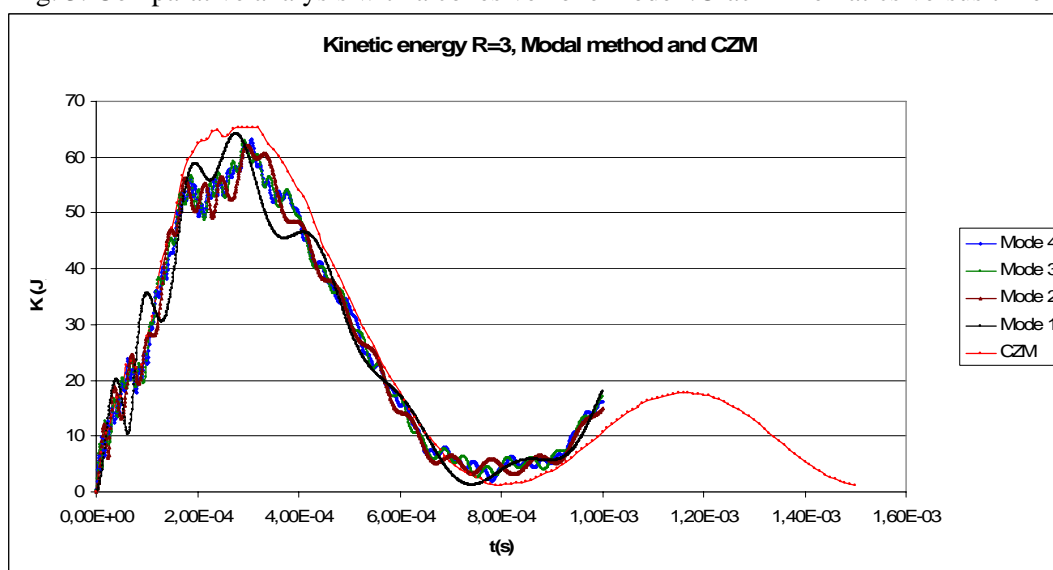


Fig. 4. Comparative analysis with a cohesive zone model :Kinetic energy versus time for  $R=3$ .

## 7. Application to materials with heterogeneous toughness .

The case of heterogeneous fracture properties is investigated, in particular when one single flaw may upset the crack kinematics. If the flaw is weaker than the safe material, the crack may jump over it. This phenomenon, called “pop-in” [8] is investigated here with the following parameters : the flaw position, and its toughness. Conversely, tougher inclusions inside the test material may slow down or stop the crack, or reduce the crack arrest length.

### 7.1. One single weak flaw ahead the initial crack tip.

In a first case, a  $e$  length single flaw, located just ahead the initial crack tip, is considered (see fig. 5). The flaw toughness value is  $\Gamma_1 = \Gamma_0 / R$  and the material recovers its original toughness  $\Gamma_0$  beyond the flaw. The aim is to check if the crack will stop just after the flaw or deeper in the original material, and in this latter case, which is the arrest length, depending of  $e$  and  $R$ .

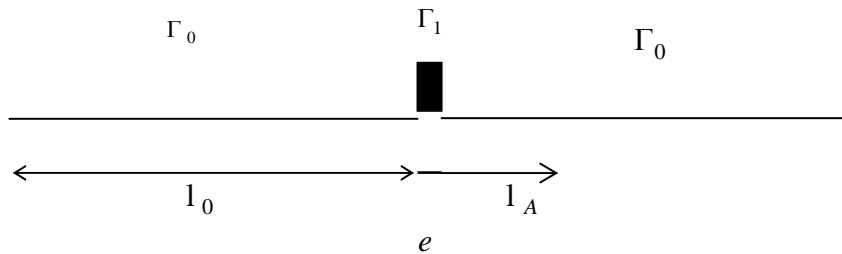


Fig. 5. One single weak inclusion ahead the initial crack tip in the test material.

The figure 6 displays the ratio crack arrest length over flaw length, versus the ratio flaw length over initial crack length, for a range of  $1.5 < R < 4$ . It is noteworthy that for  $0.2 \leq e/L_0 \leq 0.4$  (this range of  $e/L_0$  and  $R$  is usual for industrial components, the crack arrest occurs around the flaw tip, and the crack does not deeply penetrate inside the safe material.

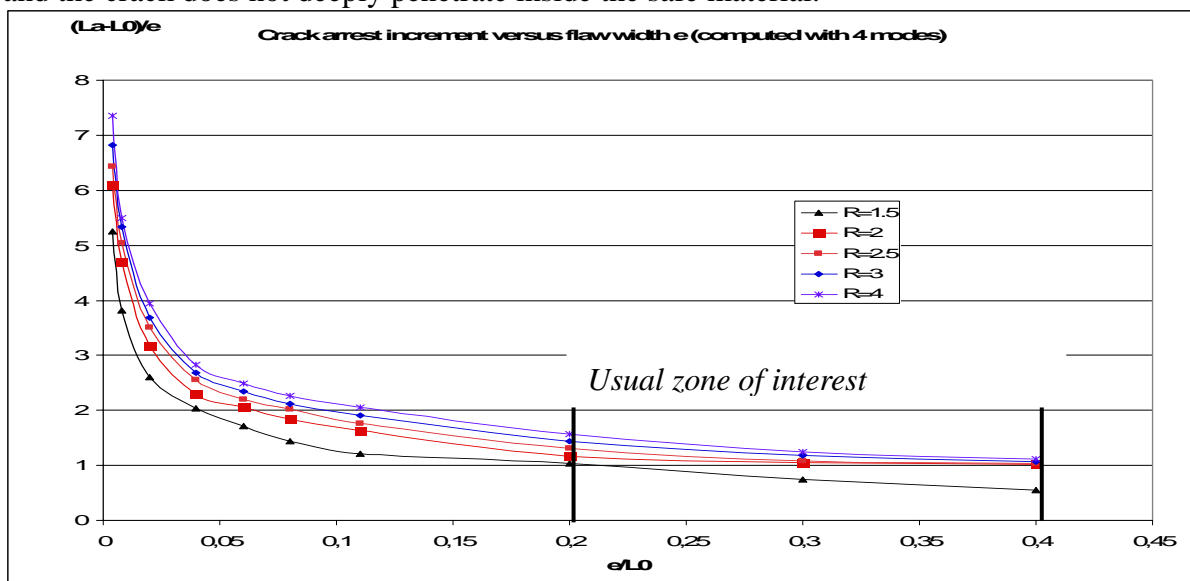


Fig. 6. Crack arrest length on flaw length, versus flaw length on initial crack length.

### 7.2. One single tough flaw ahead the initial crack tip.

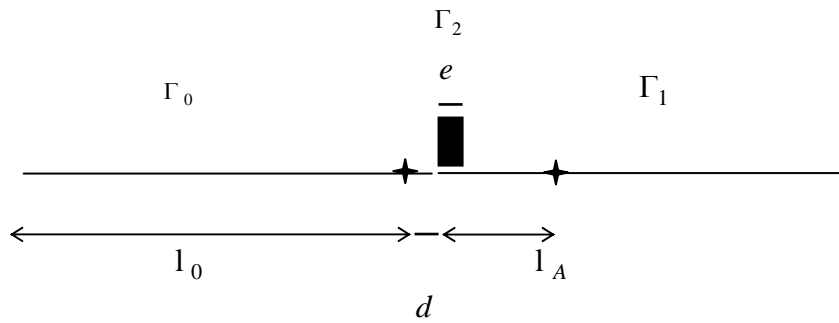


Fig. 7. One single tough inclusion in the test material.

On the contrary, a tough  $e$  length flaw ( $\Gamma_2 \geq \Gamma_0$ ) is embedded in the regular test material ( $\Gamma_1 = \Gamma_0 / R$ , with the fixed value  $R = 3$ ), at a distance  $d$  ahead the initial crack tip (fig. 7). The influence of the flaw features  $d$ ,  $e$  and  $\Gamma_2$  on the crack kinematics is investigated. If the flaw is sufficiently long (in our specific case  $e/l_0 > 6\%$ , see fig.8), the crack is immediately stopped inside the flaw. In the other hand where  $e/l_0 < 1\%$  the crack kinematics is very close to that without flaw. In the intermediate situations, a transient crack arrest takes place in the flaw (the longer the flaw, the longer the transient arrest time), followed by a crack restart with either a reduced final crack arrest (for  $e/l_0 = 5\%$ ) or a regular one (for  $e/l_0 = 3\%$ ).

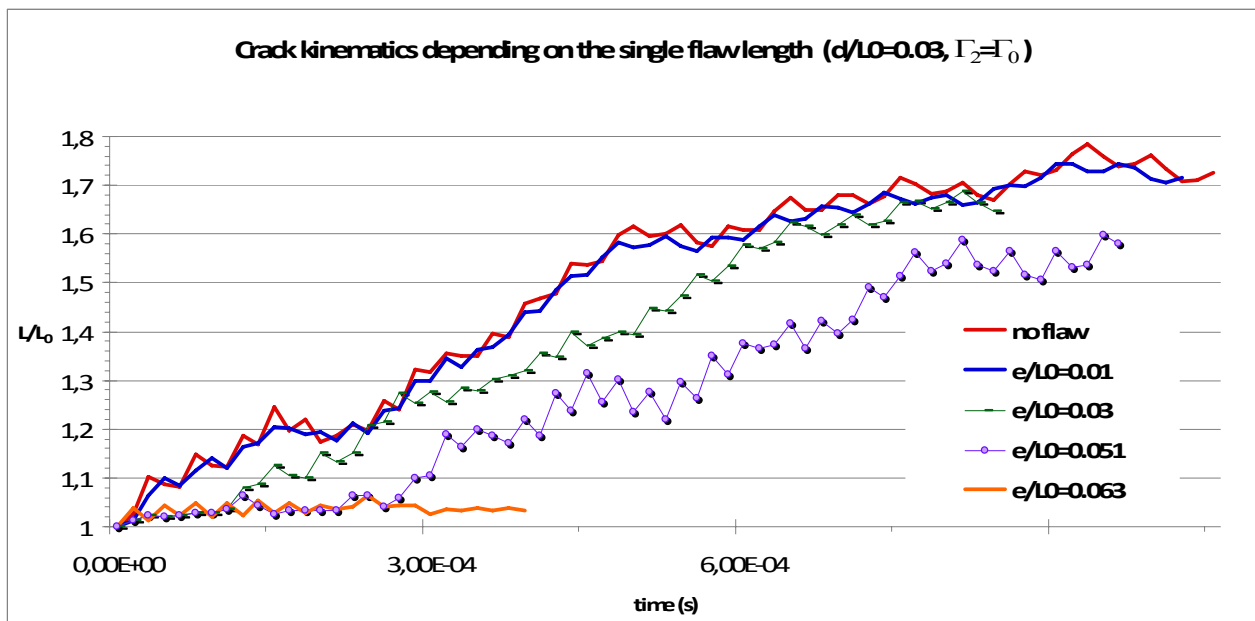


Fig. 8. Influence of the flaw length.

## 8. Conclusions and outlines.

The complete dynamic crack kinematics is described from the Hamiltonian variational formulation associated to a modal decomposition. It is correctly described in a swift time, compared to the prediction of more heavy FE methods, even for a small number of modes (in many cases, three modes are sufficient, for a few seconds of computational time). The method has been also applied to a material, embedding some flaws with heterogeneous fracture properties. The crack kinematics, including the crack arrest, is very sensitive to the flaw position and toughness. The main drawback of our method is the non account of the crack growth irreversibility, which leads to small stages with negative crack velocities instead transient crack arrest, but without significant consequence on the results fairness. This disadvantage may be circumvented, adding the constraint inequality  $\dot{P} \geq 0$  in the motion equations, but with probably an increase in the computational cost. An extension of this method to a beam with variable section geometry (tapered DCB), a complex toughness distribution, is straightforward. On the other hand, some developments concerning the material behaviour such as the viscosity or plasticity, or the application to bidimensionnal geometries are possible but more ticklish.

### References

1. N.F. Mott, Brittle fracture in mild steel plates, *Engineering* 165, pp. 16-18, 1948.
2. L.B. Freund, A simple model of the double cantilever beam crack propagation specimen, *J. Mech. Phys. Solids*, Vol. 25, pp. 69-79, 1977.
3. K. Hellan, An alternative one-dimensional study of dynamic crack growth in DCB test specimens, *Int. J. of Fracture*, Vol.17, n°3, pp. 311-319, June 1981.
4. S.J. Burns, W.W. Webb, Fracture Surface Energies and Dislocation Processes during Dynamical Cleavage of LiF. I. Theory, *J. of Applied Physics*, Vol. 41, n° 5, pp. 2078-2085, April 1970.
5. L.B. Freund, *Dynamic Fracture Mechanics*, Cambridge University Press, ISBN 0-521-30330-3, 1998 (first edition 1989).
6. V.I. Arnold, *Mathematical Methods of Classical Mechanics*, Springer Verlag, 2<sup>nd</sup> edition, pp. 59-68, 1989.
7. G. Debruyne, P.E. Dumouchel, J. Laverne, *Dynamic crack growth : Analytical and numerical Cohesive zone models approaches from basic tests to industrial structures*, *Eng. Fr. Mech.*, 2012.
8. A.A Willoughby, Significance of Pop-in fracture toughness testing, in *Int. J. of Fract.* 30, R3-R6, 1986